Transport properties of a Kondo dot with a larger side-coupled noninteracting quantum dot

2008 J. Phys.: Condens. Matter 20 135226

(http://iopscience.iop.org/0953-8984/20/13/135226)

J. Phys.: Condens. Matter **20** (2008) 135226 (7pp) doi:10.1088/0953-8984/20/13/135226

Transport properties of a Kondo dot with a larger side-coupled noninteracting quantum dot

Y S Liu[1,3], X F Yang[2], X H Fan[1] and Y J Xia[1]

[1] Physics Department, Qufu Normal University, Qufu 273165, People's Republic of China
[2] National Lab for Infrared Physics, Shanghai Institute of Technical Physics, Chinese Academy of Sciences, 500 Yutian Road, 200083 Shanghai, People's Republic of China

E-mail: ysliu2007@yahoo.com.cn

Received 23 August 2007, in final form 22 February 2008
Published 13 March 2008
Online at stacks.iop.org/JPhysCM/20/135226

Abstract

We investigate theoretically linear and nonlinear quantum transport through a smaller quantum dot in a Kondo regime connected to two leads in the presence of a larger side-coupled noninteracting quantum dot, without tunneling coupling to the leads. To do this we employ the slave boson mean field theory with the help of the Keldysh Green's function at zero temperature. The numerical results show that the Kondo conductance peak may develop multiple resonance peaks and multiple zero points in the conductance spectrum owing to constructive and destructive quantum interference effects when the energy levels of the large side-coupled noninteracting dot are located in the vicinity of the Fermi level in the leads. As the coupling strength between two quantum dots increases, the tunneling current through the quantum device as a function of gate voltage applied across the two leads is suppressed. The spin-dependent transport properties of two parallel coupled quantum dots connected to two ferromagnetic leads are also investigated. The numerical results show that, for the parallel configuration, the spin current or linear spin differential conductance are enhanced when the polarization strength in the two leads is increased.

(Some figures in this article are in colour only in the electronic version)

1. Introduction

In recent years, electronic transport through a quantum dot or molecular system has been an interesting area of research owing to advances in the nanofabrication of quantum devices [1–4]. Since the Kondo effect was first discovered in a semiconductor quantum dot experimentally [5, 6], many-body effects in nanoscale systems have been investigated theoretically and experimentally [7–11]. It is well known that the Kondo effect is a many-body singlet state arising from the creation of a spin-entangled state consisting of the localized spin state in the quantum dot and the inverse spin state in the leads. The Kondo resonance peak with the unitary limit of the conductance $G = 2e^2/h$ at the Fermi level E_F is developed at lower temperatures. The electronic tunneling becomes possible even if the quantum dot lies in the Coulomb blockage regime. The width of the Kondo conductance peak is the order of the Kondo temperature.

Fano resonance is another important interference effect in nanoscale systems, which stems from quantum interference between resonant and non-resonant processes. It was first found in atomic physics [12] and now it is studied extensively in quantum dot systems as a good probe for phase coherence [13]. An artificial molecule can be formed by coupling two (or more) quantum dots, and Kondo effects in such multiple quantum dots are studied but they are limited to single or two coupled dots. Jiang *et al* [14] studied the equilibrium and non-equilibrium Kondo transport properties of serially coupled triple quantum dots, but Fano effects cannot be observed due to the serially coupled configuration. More recently, Wu *et al* [15] studied the transport properties

[3] Author to whom any correspondence should be addressed.

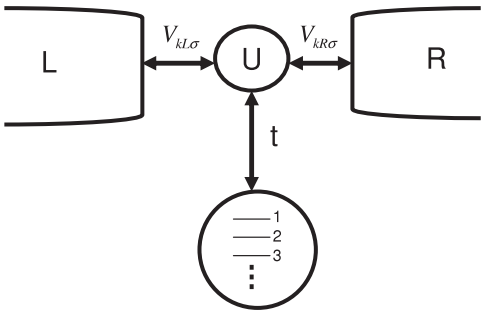

Figure 1. Schematic plot of the Kondo dot connected with the leads and a larger quantum dot without the electron–electron interactions.

of a strongly correlated quantum dot with a side-coupled noninteracting quantum dot. Two interesting problems are presented in the present work. First we look at what happens to Kondo effects when more energy levels in the side-coupled quantum dot are considered. The other problem is the spin-dependent transport through the Kondo dot when two ferromagnetic leads replace two normal metal leads. To our knowledge, less attention has been paid to Fano effects in the spin-dependent case.

In this paper, we studied electronic transport through a strongly correlated quantum dot connected to two leads in the presence of a larger side-coupled noninteracting dot by using the slave boson mean field theory (SBMFT). For low voltage and low temperature, the SBMFT has been proved to be a good method to probe the transport properties of strongly correlated systems. Spin fluctuations are only taken into account, while charge fluctuations are neglected entirely. The numerical results show that the original Kondo conductance peak may develop into a linear conductance band consisting of multiple resonances and anti-resonances due to Fano–Kondo effects when more energy levels of the large side-coupled dot are pinned around the Fermi level in the leads. The spin-dependent electric transport properties of the quantum system are also studied in the present work when a strongly correlated quantum dot is coupled to two ferromagnetic leads.

2. Model and method

The quantum device including a small quantum dot and a large quantum dot is shown schematically in figure 1, in which only the small quantum dot is coupled to the leads and the large quantum dot is coupled to the small quantum dot. Only a spin degenerate energy level in the small quantum dot is considered by tuning the shape of the small quantum dot. The electron–electron interactions in the small quantum dot become obvious, therefore the quantum dot can act as a Kondo impurity when the system temperature is low enough. The side-coupled quantum dot is assumed to be large, so the charging energy in the large quantum dot can be neglected. Multiple side-coupled transmission paths in the device are presented by using the large quantum dot. Using suitable voltages and confining the quantum dot potential [16], the energy level in the small quantum dot ϵ_d is much lower than the energy levels in the large quantum dot ϵ_j ($j = 1, \ldots$). When an infinite on-site Coulomb interaction in the small quantum dot is considered, the capacitive (interdot Coulomb interaction) coupling between the two dots may be neglected [17]. Oreg *et al* [18] suggested an experimental device consisting of a small quantum dot with a single energy level and a large quantum dot with a finite Coulomb energy. Anders *et al* [19] explored a double quantum dot system composed of a small quantum dot coupled to a quantum box (a large quantum dot) and a lead by using the numerical renormalization group method. The Kondo dot is coupled via $V_{k\alpha\sigma}$ to two Fermi-liquid reservoirs denoted by $\alpha = \{\mathrm{L}, \mathrm{R}\}$. The large quantum dot is coupled to the Kondo dot by the hopping amplitude t, and is not coupled to two reservoirs. The total Hamiltonian is given by

$$\begin{aligned} H_{\mathrm{total}} = & \sum_{k\alpha\sigma} \epsilon_{k\alpha\sigma} a^{\dagger}_{k\alpha\sigma} a_{k\alpha\sigma} + \sum_{\sigma} \epsilon_d d^{\dagger}_{\sigma} d_{\sigma} + U d^{\dagger}_{\uparrow} d_{\uparrow} d^{\dagger}_{\downarrow} d_{\downarrow} \\ & + \sum_{j\sigma} \epsilon_j c^{\dagger}_{j\sigma} c_{j\sigma} + \sum_{j\sigma} t (c^{\dagger}_{j\sigma} d_{\sigma} + \mathrm{H.c.}) \\ & + \sum_{k\alpha\sigma} (V_{k\alpha\sigma} a^{\dagger}_{k\alpha\sigma} d_{\sigma} + \mathrm{H.c.}), \end{aligned} \tag{1}$$

where $a^{\dagger}_{k\alpha\sigma}$ ($a_{k\alpha\sigma}$) is the creation (annihilation) operator for an electron with energy $\epsilon_{k\alpha\sigma}$ and spin index σ in lead α; $d^{\dagger}_{\sigma}(d_{\sigma})$ creates (destroys) an electron with spin index σ in the Kondo dot; $c^{\dagger}_{j\sigma}(c_{j\sigma})$ represents the creation (annihilation) operator for an electron with spin index σ in the jth energy level inside the larger quantum dot. U is the on-site energy scale in the Kondo impurity. The energy levels of the larger quantum dot are chosen as

$$\epsilon_j = \epsilon_1 - (j-1)\Delta \qquad (j = 2, 3, \ldots), \tag{2}$$

where ϵ_1 is the first energy level inside the larger quantum dot, and Δ denotes the difference between two nearest energy levels. When the intradot Coulomb interaction is sufficiently large, the double occupied state inside the Kondo dot is forbidden. Using the slave-boson representation, the annihilation (creation) operator d_{σ} ($d^{\dagger}_{\sigma}$) in the Kondo dot is represented by $d_{\sigma} = b^{\dagger} f_{\sigma}$ ($d^{\dagger}_{\sigma} = f^{\dagger}_{\sigma} b$) with boson field b and pseudofermion field f_{σ}, which implies that destroying an electron in the Kondo dot is equivalent to destroying a pseudoelectron with spin σ and creating a boson at the same time. The two-fold degenerate Anderson Hamiltonian with the Lagrange multiplier λ is rewritten as

$$\begin{aligned} \tilde{H}_{\mathrm{total}} = & \sum_{k\alpha\sigma} \epsilon_{k\alpha\sigma} a^{\dagger}_{k\alpha\sigma} a_{k\alpha\sigma} + \sum_{\sigma} \epsilon_d f^{\dagger}_{\sigma} f_{\sigma} + \sum_{j\sigma} \epsilon_j c^{\dagger}_{j\sigma} c_{j\sigma} \\ & + \frac{1}{\sqrt{N}} \sum_{j\sigma} t (c^{\dagger}_{j\sigma} b^{\dagger} f_{\sigma} + \mathrm{H.c.}) \\ & + \frac{1}{\sqrt{N}} \sum_{k\alpha\sigma} (V_{k\alpha\sigma} a^{\dagger}_{k\alpha\sigma} b^{\dagger} f_{\sigma} + \mathrm{H.c.}) \\ & + \lambda \left(\sum_{\sigma} f^{\dagger}_{\sigma} f_{\sigma} + b^{\dagger} b - 1 \right). \end{aligned} \tag{3}$$

In the lowest order, we assume that the slave-boson (SB) operator is a constant real number $b(t)/\sqrt{N} = \tilde{b}$ and neglect the fluctuations around the average $\langle b(t) \rangle$. At zero temperature, this SBMFT is reasonable for describing

spin fluctuations (Kondo regime), which restricts our non-equilibrium calculation to low voltages $V \ll \epsilon_d$. Equation (3) is rewritten as

$$\tilde{H}_{\rm total} = \sum_{k\alpha\sigma} \epsilon_{k\alpha\sigma} a^\dagger_{k\alpha\sigma} a_{k\alpha\sigma} + \sum_{\sigma} \tilde{\epsilon}_d f^\dagger_\sigma f_\sigma + \sum_{j\sigma} \epsilon_j c^\dagger_{j\sigma} c_{j\sigma} + \tilde{t} \sum_{j\sigma} (c^\dagger_{j\sigma} f_\sigma + \text{H.c.}) + \sum_{k\alpha\sigma} (\tilde{V}_{k\alpha\sigma} a^\dagger_{k\alpha\sigma} f_\sigma + \text{H.c.}) + \lambda \left(N\tilde{b} - 1 \right), \quad (4)$$

where $\tilde{\epsilon}_d = \epsilon_d + \lambda$. Using the constraints and the equation of motion of the SB operator $\frac{\rm d}{{\rm d}t}\langle \tilde{b} \rangle = 0$, the two self-consistent equations with two unknowns $(\tilde{b}, \lambda)$ can be written as

$$2\tilde{b}^2 + \sum_\sigma n_{f\sigma} = 1 \quad (5)$$

and

$$\lambda \tilde{b}^2 - {\rm i} \sum_\sigma \int \frac{{\rm d}\epsilon}{4\pi} (\epsilon - \tilde{\epsilon}_d) G^<_{f\sigma}(\epsilon) = 0, \quad (6)$$

where $G^<_{f\sigma}(\epsilon)$ denotes the lesser Green's function of the Kondo dot and $n_{f\sigma}$ is the electron occupation number at the quantum state $\tilde{\epsilon}_d$ in the presence of the Kondo correlations. Once the retarded Green's function of the Kondo dot is achieved, the lesser Green's function can be obtained by the Keldysh equation

$$G^<_{f_\sigma}(\epsilon) = G^{\rm r}_{f\sigma}(\epsilon) \tilde{\Sigma}^<_\sigma(\epsilon) G^{\rm a}_{f\sigma}(\epsilon), \quad (7)$$

where $\tilde{\Sigma}^<_\sigma = 2{\rm i}[\tilde{\Gamma}^{\rm L}_\sigma f_{\rm L}(\epsilon) + \tilde{\Gamma}^{\rm R}_\sigma f_{\rm R}(\epsilon)]$, and the Fermi–Dirac distribution function for the αth electrode is $f_\alpha(\epsilon) = 1/\{1 + \exp[(\epsilon - \mu_\alpha)/k_{\rm B}T]\}$ with the electrochemical potential $\mu_{\rm L} = eV/2$ and $\mu_{\rm R} = -eV/2$, where the bias V is applied across two leads. $\tilde{\Gamma}^\alpha_\sigma = \tilde{b}^2 \Gamma^\alpha_\sigma$ describes the renormalized linewidth function to the lead α. In the wide band limit, the noninteracting line with $\Gamma^\alpha_\sigma = \sum_k \pi |V_{k\alpha\sigma}|^2 \delta(\epsilon - \epsilon_{k\alpha\sigma})$ is regarded as the energy-independent constant. Using the equation-of-motion for the operator f_σ, we obtain the retarded Green's function

$$G^{\rm r}_{f_\sigma}(\epsilon) = \frac{\prod_j (\epsilon - \epsilon_j)}{(\epsilon - \tilde{\epsilon}_d + {\rm i}\tilde{\Gamma}_\sigma) \prod_j (\epsilon - \epsilon_j) - \sum_j \tilde{t}^2 \prod_{j'} (\epsilon - \epsilon_{j'})/(\epsilon - \epsilon_j)}, \quad (8)$$

where $\tilde{\Gamma}_\sigma = \tilde{\Gamma}^{\rm L}_\sigma + \tilde{\Gamma}^{\rm R}_\sigma$, and $G^{\rm r}_{f\sigma}(\epsilon)$ is the Fourier transform of the retarded Green's function $G^{\rm r}_{f\sigma}(t, t') = -{\rm i}\theta(t - t')\langle\{f_\sigma(t), f^\dagger_\sigma(t')\}_+\rangle^{\rm r}$.

By using the renormalized parameters determined self-consistently, the tunneling current through the system is given by the Landauer–Büttiker form [20–22]

$$I = \frac{e}{h} \sum_\sigma \int {\rm d}\epsilon [f_{\rm L}(\epsilon) - f_{\rm R}(\epsilon)] \tilde{T}_\sigma(\epsilon), \quad (9)$$

with the left/right Fermi–Dirac distribution function $f_{L/R}(\epsilon)$. The transmission probability $\tilde{T}_\sigma(\epsilon)$ for spin index σ with energy ϵ is

$$\tilde{T}_\sigma(\epsilon) = \frac{2\tilde{\Gamma}^{\rm L}_\sigma \tilde{\Gamma}^{\rm R}_\sigma}{\tilde{\Gamma}^{\rm L}_\sigma + \tilde{\Gamma}^{\rm R}_\sigma} A_\sigma(\epsilon). \quad (10)$$

$A_\sigma(\epsilon)$ is the spectral function with spin σ, which is defined as

$$A_\sigma(\epsilon) = {\rm i}[G^{\rm r}_{f\sigma}(\epsilon) - G^{\rm a}_{f\sigma}(\epsilon)]. \quad (11)$$

The differential conductance $G = {\rm d}I/{\rm d}V$ is calculated from equation (9). From the above results, we note that the transport properties depend implicitly on $\tilde{b}$ and λ, which must be calculated self-consistently when system parameters are given. Such a feature results in some interesting effects, which are not observed in the noninteracting Anderson model [23–25].

3. Results and discussion

In this section, we will present the numerical results using Lorentzian bands with $D = 60\Gamma$. The bare level for the Kondo impurity is fixed at $\epsilon_d = -3.5\Gamma$ with $\Gamma = \Gamma^\alpha_\uparrow + \Gamma^\alpha_\downarrow$ $(\alpha = {\rm L}, {\rm R})$, and Γ is taken as the energy unit. In the following calculation we consider the case when the Fermi level is pinned at zero energy ($E_{\rm F} = 0$).

3.1. Non-polarized leads

We first study the transport properties of the double-dot system for the equilibrium case when the bias voltage V is infinitesimally small. The linear differential conductance G can be calculated readily by using equation (9) once $\tilde{b}$ and λ are obtained self-consistently. In figure 2(a), we plot the differential conductance G as a function of the gate voltage $V_{\rm g}$ applied to the larger quantum dot including three energy levels at zero temperature. Due to the Fermi energy level fixed at zero energy ($E_{\rm F} = 0$), the transmission coefficient for spin index σ can be approximated by

$$\tilde{T}_\sigma(\epsilon_1) \approx 4\tilde{\Gamma}^{\rm L}_\sigma \tilde{\Gamma}^{\rm R}_\sigma \frac{(\prod_j \epsilon_j)^2}{(\sum_j \tilde{t}^2 \prod_{j'} \epsilon_{j'}/\epsilon_j)^2 + \tilde{\Gamma}^2_\sigma (\prod_j \epsilon_j)^2}. \quad (12)$$

In the following, we study the linear transport properties of a quantum system, in which the larger quantum dot includes three energy levels. A gate voltage $V_{\rm g}$ is applied to the larger quantum dot, which induces the energy levels inside the larger quantum dot to shift together. The level spacing in the larger quantum dot Δ is fixed at $0.5T_{\rm K}$, in which $T_{\rm K} = D{\rm e}^{-\pi|\epsilon_d - E_{\rm F}|/\Gamma}$ denotes the Kondo temperature at equilibrium when the coupling between the Kondo dot and the large quantum dot is absent. In experiments, we can control the number and the level spacing of the energy levels in the larger quantum dot by tuning the shapes of the larger quantum dot. For simplicity, the levels can be considered as equidistant in our model. For $|V_{\rm g}| \gg E_{\rm F}$, the quantum transport through the Kondo dot is not affected by the larger side-coupled noninteracting quantum dot, therefore the maximal differential conductance $G = 2e^2/h$ is obtained due to the Kondo effect. Three anti-resonant dips appear at 0, Δ, and 2Δ due to the destructive quantum interference, and two resonant peaks appear around $(1 \pm \frac{\sqrt{3}}{3})\Delta$ due to the constructive quantum interference effect. As the tunneling rate between two dots becomes small, the transport properties of two dots are mainly dependent on the Kondo effect, and the Fano effect becomes inconspicuous. The two conductance peaks become wider,

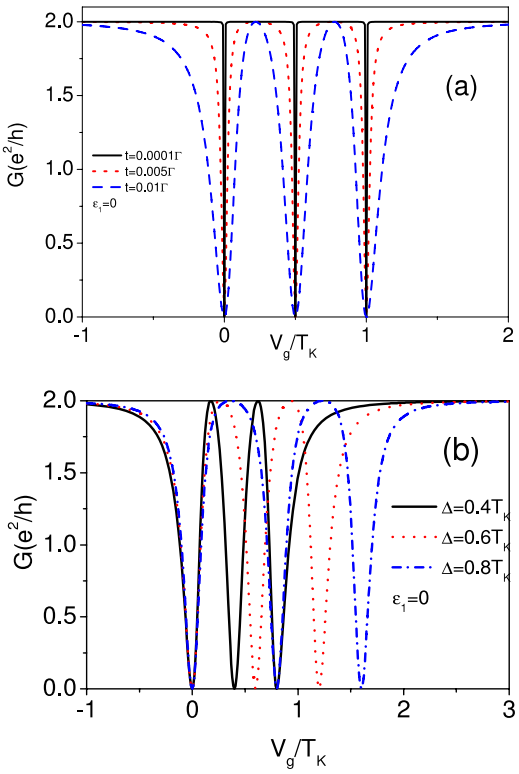

Figure 2. Differential conductance G of the quantum dot molecule as a function of gate voltage V_g applied to the larger quantum dot. (a) The coupling strength between the Kondo dot and the side-coupled dots t is chosen as 0.001Γ (solid line), 0.005Γ (dotted line), and 0.01Γ (dashed line), respectively. (b) The level spacing in the large quantum dot Δ is chosen as $0.4T_K$ (solid line), $0.6T_K$ (dotted line), and $0.8T_K$ (dashed line), respectively.

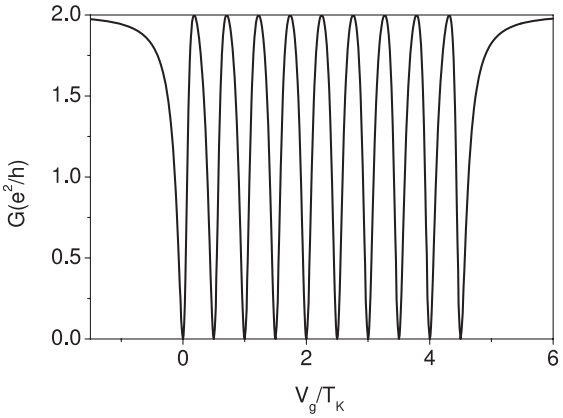

Figure 3. Differential conductance G as a function of the gate voltage V_g applied to the larger quantum dot with ten quantum dot energy levels.

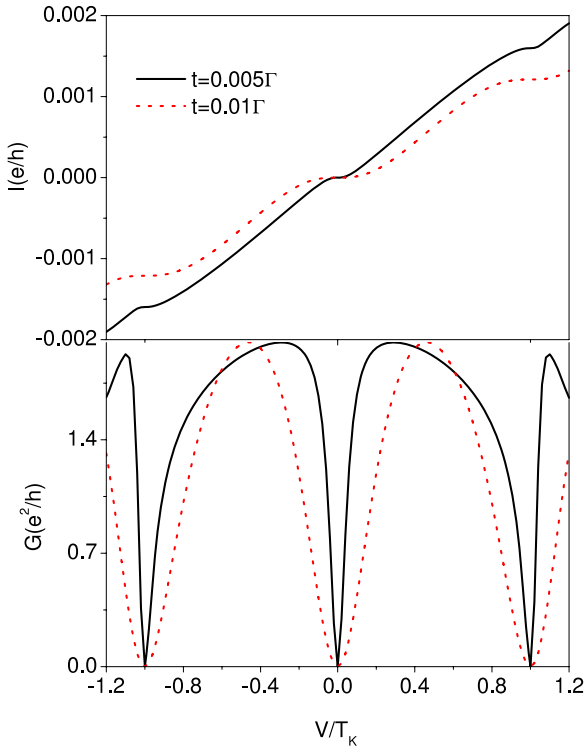

Figure 4. Differential conductance G and tunneling current I as functions of bias V with different tunneling couplings. The solid line corresponds to the case with $t = 0.005\Gamma$ and the dotted line corresponds to the case with $t = 0.01\Gamma$.

while the anti-resonance points stay at the original positions. In figure 2(b), the differential conductance G as a function of the gate voltage V_g under several different level spacings at zero temperature is plotted. The interdot tunneling coupling is taken as $t = 0.01\Gamma$. The results show that the anti-resonant dips ($G = 0$) are dependent on the level spacings. When more energy levels inside the larger quantum dot are considered, there are more anti-resonances and resonances emerge in the differential conductance curve. Figure 3 shows the behavior of the linear conductance as a function of V_g when ten energy levels inside the larger quantum dot are considered. Due to multiple Fano–Kondo interactions, we find that ten anti-resonant dips and nine resonant peaks appear in the linear conductance spectrum.

Now let us pay some attention to the transport behavior of the quantum dot molecule in the non-equilibrium case by using equation (9). In figure 4, we plot the tunneling current through the quantum dot molecule and the corresponding nonlinear differential conductance as functions of the lower applied bias V with parameters $\epsilon_1 = 0.5T_K$ and $\Delta = 0.5T_K$ on the top and low plane under different coupling strengths between the Kondo impurity and the larger side-coupled noninteracting quantum dot including three energy levels. In the absence of the larger quantum dot $t = 0$, only the Kondo dot takes part in transporting through the quantum device. The maximal differential conductance $\frac{2e^2}{h}$ at zero bias is always observed due to Kondo effects, which are studied widely using various approaches. In this work, we pay attention to the case when a larger quantum dot, including multiple energy levels, is attached to the Kondo dot. The results show that the zero bias anomaly may be entirely suppressed when one of the multiple energy levels is aligned with Fermi energy $E_F = 0$. Due to constructive quantum interference we observed several differential conductance peaks related to the smooth increasing of tunneling current through the quantum system, and due

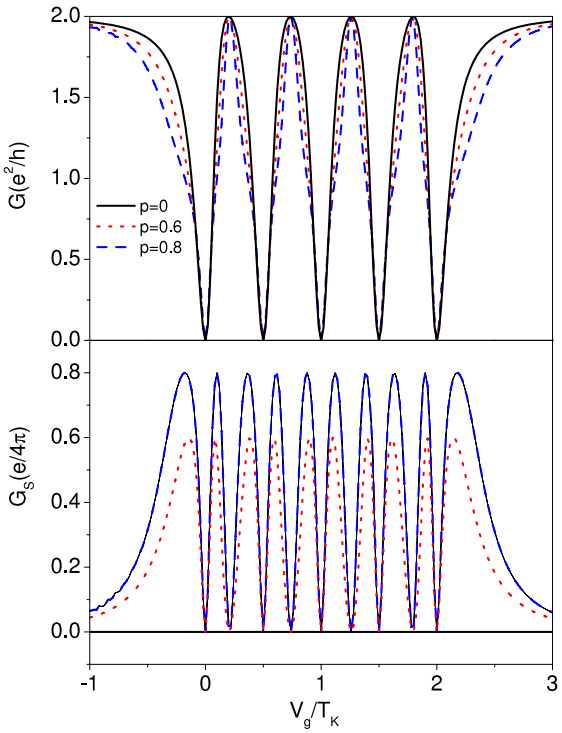

Figure 5. The charge differential conductance G and spin differential conductance G_S as functions of the gate voltage V_g applied to the larger quantum dot. (a) The charge conductance for the parallel configuration. (b) The spin conductance for the parallel configuration. The coupling strength between the two quantum dots is chosen as $t = 0.01\Gamma$.

to destructive quantum interference we observed several zero conductance points around $V = \pm 2\epsilon_j$. As t increases, the tunneling current through the system decreases.

3.2. Polarized leads

In this section, we will consider two kinds of magnetic configurations: (i) the parallel (P), where the majority of electrons at the left electrode and the right electrode are in the same directions; and (ii) the antiparallel (AP), where the magnetization of the right electrode is reversed. It is well known that the coherent spin transport parameters can be conveniently expressed by introducing magnetic polarization factors p for the polarized leads. For P configuration, $\Gamma^{\rm L}_{\uparrow} = \Gamma^{\rm R}_{\uparrow} = (1+p)\Gamma/2$ and $\Gamma^{\rm L}_{\downarrow} = \Gamma^{\rm R}_{\downarrow} = (1-p)\Gamma/2$. For AP configuration $\Gamma^{\rm L}_{\uparrow} = \Gamma^{\rm R}_{\downarrow} = (1+p)\Gamma/2$ and $\Gamma^{\rm L}_{\downarrow} = \Gamma^{\rm R}_{\uparrow} = (1-p)\Gamma/2$, where p denotes the polarization strength of the two leads.

Let us first analyze the electronic transport through the Kondo dot attached to the parallel configuration of the polarized leads under several different values of p at zero temperature. The system parameter Δ is chosen to be $0.5T_{\rm K}$. In figure 5, we plot the charge differential conductance G and spin differential conductance $G_{\rm s}$ as functions of the gate voltage $V_{\rm g}$ applied to the larger noninteracting quantum dot including five energy levels under infinitesimally small bias. G is calculated by equation (9), and $G_{\rm s}$ can be obtained by the following

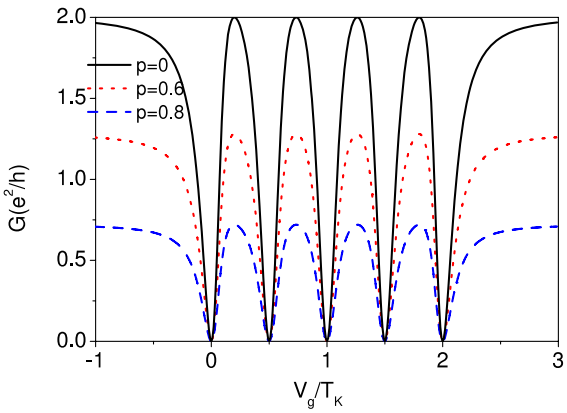

Figure 6. Charge differential conductance as a function of the gate volatage $V_{\rm g}$ for the antiparallel case for several different values of p. Other parameters are chosen as in figure 5.

equation $G_{\rm s} = {\rm d}I_{\rm S}/{\rm d}V$, where the spin current is given by using the relation $I_{\rm S} = \frac{\hbar}{2e}(I_{\uparrow} - I_{\downarrow})$. This definition of the spin current has been adopted in some works [26, 27]. As a result of the destructive quantum interference effects, five anti-resonant points appear around 0, Δ, 2Δ, 3Δ and 4Δ, respectively. Four resonant peaks emerge in the middle regions of every two anti-resonant dips due to the constructive quantum interference effects. The charge differential conductance curve becomes narrower with the increase of p, however the heights of these conductance peaks are always at the unitary limit $2e^2/h$. The reason for this is that the same tunneling couplings for the up-spin and down-spin electrons $\Gamma^{\rm L}_{\uparrow} = \Gamma^{\rm R}_{\uparrow}$ and $\Gamma^{\rm L}_{\downarrow} = \Gamma^{\rm R}_{\downarrow}$ exist when the parallel configuration is presented, which results in the heights of the main conductance peaks being almost independent of p. In the spin differential conductance $G_{\rm s}$ curves, we find that some new zero spin conductance points appear at the positions of the charge conductance peaks due to $I_{\uparrow} = I_{\downarrow}$. So nine zero spin conductance dips appear in the double quantum dot system. As p increases, the spin conductance peaks become higher and broader due to $\Gamma^{\rm L}_{\uparrow} + \Gamma^{\rm R}_{\uparrow} > \Gamma^{\rm L}_{\downarrow} + \Gamma^{\rm R}_{\downarrow}$. For the antiparallel configuration, up-spin and up–down electrons have asymmetry tunneling couplings for the left and right electrode $\Gamma^{\rm L}_{\uparrow} > \Gamma^{\rm R}_{\uparrow}$ and $\Gamma^{\rm L}_{\downarrow} < \Gamma^{\rm R}_{\downarrow}$. So we see that the linear charge differential conductance as a function of the applied gate voltage $V_{\rm g}$ in figure 6 decreases as p increases. Due to $I_{\uparrow} = I_{\downarrow}$ for the antiparallel case, the spin differential conductance of the quantum dot molecule disappears in the quantum system.

Finally, we consider the non-equilibrium transport properties of the quantum system in figure 7. We plot the charge current and spin current as functions of the applied voltage V across the leads under several different values of p for the parallel configuration, in which the larger quantum dot includes three quantum energy levels. The system parameters are chosen to be $\epsilon_1 = 0.5T_{\rm K}$ and $\Delta = 0.5T_{\rm K}$, respectively. In the high voltage region, the dependence of the charge current on p becomes obvious, and it decreases monotonically with the increase of p. The spin current exhibits the inverse behavior as p increases. Due to the Fano–Kondo interaction, we find that several steps appear in the charge curve, while more

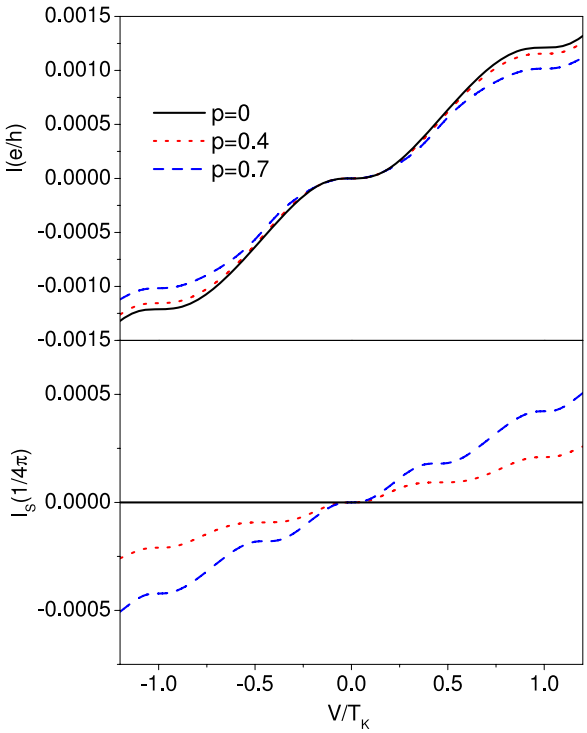

Figure 7. The charge current I and spin current I_S through the quantum system as functions of the applied volatage V for the parallel case. The coupling strength between two quantum dots is chosen as $t = 0.01\Gamma$. Other system parameters are chosen as in figure 4.

steps emerge in the spin current curve. Figure 8 shows the dependence of the charge current on the applied voltage under several different values of p for the antiparallel configuration. The results shows that the charge current decreases with the increase of p for the antiparallel configuration when the applied voltage is fixed.

4. Summary

In summary, we have studied theoretically the transport properties of a Kondo quantum dot coupled to two leads and to a side-coupled larger noninteracting quantum dot without tunneling coupling to the leads. To do this we have used the slave boson mean field theory with the help of the Keldysh Green's function at zero temperature. As a consequence of the Fano–Kondo interactions, the linear and nonlinear conductance spectra exhibit an oscillating band with the resonances and anti-resonances when the energy levels of the side-coupled large quantum dot are located around the Fermi level in the leads. As the coupling strength between two quantum dots increases, the tunneling charge current through the quantum dots system is suppressed. Spin-dependent transport properties of a Kondo dot connected with two ferromagnetic leads are also studied in this paper. Spin current through two quantum dots is calculated numerically for the parallel configuration. The results show that spin current or linear spin differential conductance are enhanced with increase of p. We also studied

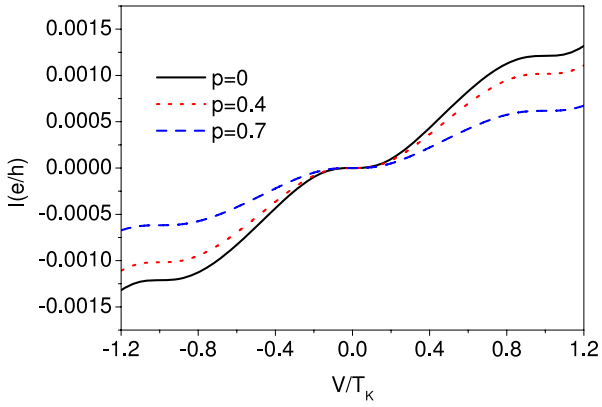

Figure 8. The charge current I through the quantum system as a function of the applied volatage V for the antiparallel case under several different values of p. Other parameters are chosen as in figure 7.

the charge current and differential conductance for parallel and antiparallel configurations.

Acknowledgments

One of the authors (Y S Liu) would like to thank Dr B H Wu for useful discussions. The work is financially supported by the National Natural Science Foundation of China (NSFC) under Grant No. 1077408.

References

[1] Liang W, Bockrath M and Park H 2002 *Phys. Rev. Lett.* **88** 126801
[2] For a review see for example Vanderwiel W G, Franceschi S D, Elgerman J M, Tarucha S and Kouwenhoven L P 2003 *Rev. Mod. Phys.* **75** 1
[3] Liu Y S, Chen H, Fan X H and Yang X F 2006 *Phys. Rev.* B **73** 115310
[4] Liu Y S, Chen H and Yang X F 2007 *J. Phys.: Condens. Matter* **19** 246201
[5] Goldhaber-Gordon D, Shtrikman H, Mahalu D, Abusch-Magder D, Meirav U and Kastner M A 1998 *Nature* **391** 156
[6] Goldhaber-Gordon D, Göres J, Kastner M A, Shtrikman H, Mahalu D and Meirav U 1998 *Phys. Rev. Lett.* **81** 5225
[7] Sasaki S, Franceschi S De, Elzerman J M, van der Wiel W G, Eto M, Tarucha S and Kouwenhoven L P 2000 *Nature* **405** 764
[8] Ji Y, Heiblum M, Sprinzak D, Mahalu D and Shtrikman H 2000 *Science* **779** 290
[9] Ji Y, Heiblum M and Shtrikman H 2002 *Phys. Rev. Lett.* **88** 076601
[10] Krawiec M and Wysokiński K I 2002 *Phys. Rev.* B **66** 165408
[11] Świrkowicz R, Barnaś J and Wilczyński1 M 2003 *Phys. Rev.* B **68** 195318
[12] Fano U 1961 *Phys. Rev.* **124** 1866
[13] Clerk A A, Waintal X and Brouwer P W 2001 *Phys. Rev. Lett.* **86** 4636
[14] Jiang Z T, Sun Q F and Wang Y P 2005 *Phys. Rev.* B **72** 045332
[15] Wu B H, Cao J C and Ahn K H 2005 *Phys. Rev.* B **72** 165313
[16] Huttel A K, Ludwig S, Lorenz H, Eberl K and Kotthaus J P 2005 *Phys. Rev.* B **72** 081310

[17] Güçlü A D, Sun Q F and Guo H 2003 *Phys. Rev.* B **68** 245323
[18] Oreg Y and Goldhaber-Gordon D 2003 *Phys. Rev. Lett.* **90** 136602
[19] Anders F B, Lebanon E and Schiller A S 2005 *Physica* B **359** 1381
[20] Meir Y and Wingreen N S 1992 *Phys. Rev. Lett.* **68** 2512
[21] Meir Y, Wingreen N S and Lee P A 1991 *Phys. Rev. Lett.* **66** 3048
[22] Meir Y, Wingreen N S and Lee P A 1993 *Phys. Rev. Lett.* **70** 2601
[23] Aguado R and Langreth D C 2000 *Phys. Rev. Lett.* **85** 1946
[24] López R, Aguado R and Platro G 2004 *Phys. Rev.* B **69** 235305
[25] Sánchez D and López R 2005 *Phys. Rev.* B **71** 035315
[26] Wang D K, Sun Q F and Guo H 2004 *Phys. Rev.* B **69** 205312
[27] Wang B, Zhu Y, Ren W, Wang J and Guo H 2007 *Phys. Rev.* B **75** 235415